Chaotic Optical Communication over Turbulent Channel

L. Illing*, N. F. Rulkov* and M. A. Vorontsov†

*Institute for Nonlinear Science, University of California, San Diego, La Jolla, CA 93093-0402
†Army Research Laboratory, Adelphi, Maryland 20783

Abstract. We experimentally demonstrate robust self-synchronizing chaos based communication over an approximately 5km free-space laser link operating in a turbulent environment. A binary information sequence is transmitted using a chaotic sequence of short-term pulses and Chaotic Pulse Position Modulation (CPPM), where each pulse is slightly shifted from the original chaotic time position depending on the transmitted binary bit. We report the results of an experimental analysis of the atmospheric turbulence in the channel and the Bit-Error-Rate (BER) performance of this chaos based communication system. The dynamics of error bursts in the CPPM communication system caused by the atmospheric turbulence is discussed.

INTRODUCTION

Thanks to the chaotic origin of chaos, two coupled chaotic oscillators can be synchronized (self-synchronized) to reproduce at the receiver end the chaotic signals generated at the transmitter [1]. Exploiting self-synchronization information encoded in the received chaotic signal can be recovered [2], thereby allowing the use of chaotic carriers for information transmission. Chaos communications is of broad interest because it both enlarges the design possibilities of communication systems and it provides a challenge due to the complexity of nonlinear dynamical issues involved [3].

All practical communication channels will distort the chaotic waveform shape so that the received signal deviates from the transmitter oscillations. Channel noise, filtering, attenuation variability and other distortions in the channel corrupt the carrier and information signal. The presence of distortions can severely degrade the quality and significantly hamper the onset of identical synchronization [4]. Above a critical level of signal distortion self-synchronization fails completely resulting in a loss of the communication link.

A number of special methods have been proposed to overcome the problem of enhanced sensitivity to signal distortions found in communication schemes based on chaos synchronization, thereby removing what is still considered one of the major obstacles for practical implementation of chaos-based communication schemes [5]. At least in theory and numerical simulations, it appears that the regime of identical synchronization in these specially designed systems is significantly less sensitive to channel noise and waveform distortions caused by limited bandwidth of the channel [6]. However, to the best of our knowledge, robust self-synchronizing chaos communication over a channel with significant non-stationary signal distortions has not been demonstrated so far.

CP676, *Experimental Chaos: 7th Experimental Chaos Conference,*
edited by V. In, L. Kocarev, T. L. Carroll, B. J. Gluckman, S. Boccaletti, and J. Kurths

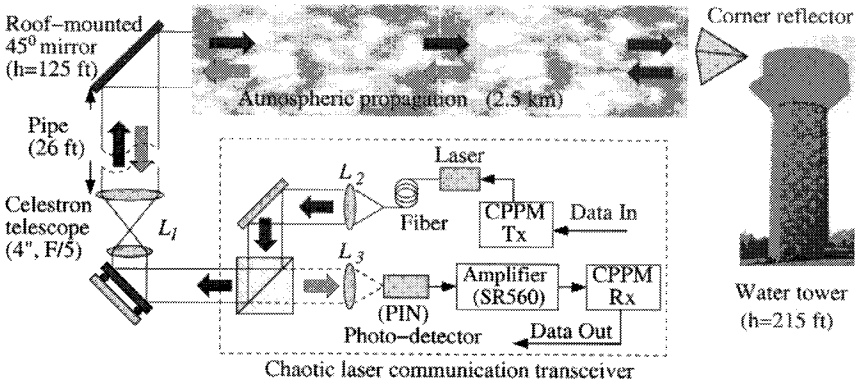

FIGURE 1. Schematic experimental setup for free-space laser communication system with chaotic pulse position modulation transceiver

Here we report the first experimental study of a chaotic self-synchronizing free-space laser communication system operating in the presence of severe communication signal distortions caused by atmospheric turbulence.

The experimental setup is schematically shown in Fig. 1. CPPM Tx and CPPM Rx represent the analog circuit implementation of the Chaotic Pulse Position Modulation transceiver. The optical part of the experiment consisted of an intensity-modulated semiconductor laser beam (10 mW, $\lambda = 690$ nm) that propagated by means of a single-mode fiber, a lens relay system (lenses L_1 and L_2) and telescope (Celestrone), which expanded the beam to a 4" diameter, and a 26 ft long vertical air-locked pipe to a 45° roof-mounted mirror. The light subsequently traveled over an atmospheric path of length $L = 2.5$km to a 4" corner cube mounted on top of a water tower, where it was reflected and propagated back to the roof-mounted mirror. The receiver system used the same telescope and lens relay system as the transmitter. The total double-pass atmospheric laser beam propagation distance was approximately $L \approx 5$km.

TURBULENT CHANNEL

Turbulence in the atmospheric communication channel leads to severe laser beam intensity scintillations that result in deep fluctuations of the received communication signal (received laser beam power). Double-pass wave propagation as in our experiment amplifies these fluctuations due to backscatter enhancement effects [7]. The most deleterious effects from receiver plane scintillations are the loss of signal-to-noise ratio and drop-outs (information loss).

To evaluate the level of intensity scintillations in the atmospheric channel we measured the received signal from a continuously running laser with constant output intensity. Figure 2a shows the fluctuations of the normalized received power, measured by the PIN photodetector placed in the lens L_3 focal plane (Fig. 1), amplified by the low noise preamplifier (SR500 with gain of 20), and then acquired with sampling rate 1000 sam-

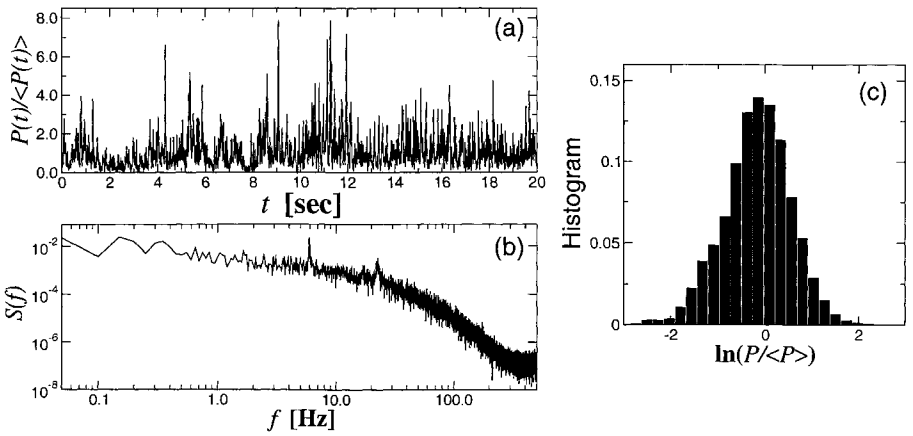

FIGURE 2. Fluctuations of the received power $P(t)$ in the experiment with non-modulated laser generating constant output intensity (10mW). Normalized received power $P(t)/\langle P(t)\rangle$ measured at the photodetector output - (a), and corresponding averaged power spectrum of - (b) illustrate the presence of strong laser beam intensity scintillations. c) Histogram of the probability distribution for the random variable $\ln(P/\langle P\rangle)$.

ples/sec. The received signal standard deviation is as high as 0.8-0.9, which is indicative of a strong scintillation regime. The corresponding ensemble-averaged received signal power spectrum S is shown in Fig. 2b.

In atmospheric optics the laser beam scintillations are traditionally described in terms of the logarithm of the received power (for finite receiver telescope): $\ln(P/\langle P\rangle)$, where $\langle P\rangle$ is the ensemble (time) averaged value [8]. A histogram that represents the distribution of the values of the random variable $\ln(P/\langle P\rangle)$ normalized by the total number of samples is shown in Fig. 2c. The histogram is computed using $N = 10^5$ consecutive samples of the data $P(t)$, a 20 sec segment of which is shown in Fig. 2a. Representing an approximation to the probability distribution of the received power the histogram closely matches the log-normal distribution expected from theory [8].

FREE-SPACE COMMUNICATION

In the communication experiment the laser generated a chaotic sequence of short term pulses ($\sim 1.0\mu s$) that were triggered by a TTL pulse signal from the chaotic transceiver controller CPPM Tx (see Fig. 1). The chaotic sequence of time intervals $\{T_n\}$, where T_n is the time interval between the nth and the $(n-1)$th pulse, corresponds to iterations of a chaotic process with the binary information signal added to the chaotic signal. This method of chaos communication is referred to as Chaotic Pulse Position Modulation (CPPM) [10]. Since both chaos and information are in the timing of the pulses, the particular intensity waveform of the generated light pulses is of little consequence.

In the implementation of CPPM discussed here the chaos is produced by iterations of a one-dimensional tent map (see [10] for details on the design). Denoting with $F(\cdot)$ the

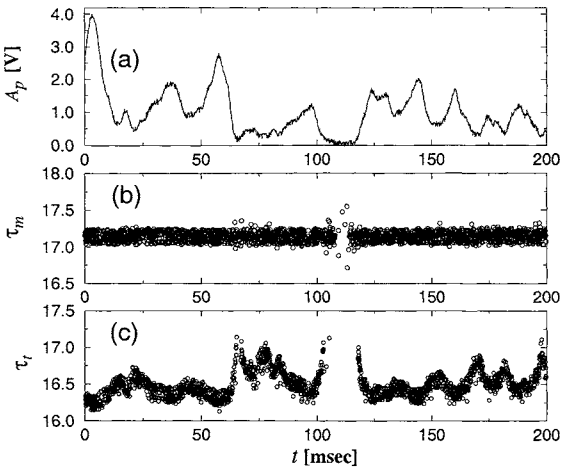

FIGURE 3. Fluctuations of the CPPM light pulses after traveling through atmospheric turbulence. Pulse amplitude A_p measured in volts at the output of amplifier - (a). Propagation times τ_m - (b) and τ_t - (c) in μsec. The pulse propagation times are computed from data acquired simultaneously at the output of CPPM Tx and output of Amplifier (SR560) at a sampling rate of 5×10^6 samples per sec.

nonlinear function of the tent map and with S_n the nth binary information signal (zero or one) we can write the iterative map that generates the chaotic sequence of time intervals $\{T_n\}$ as

$$T_n = F(T_{n-1}) + d + mS_n. \tag{1}$$

The parameter m signifies the modulation amplitude, whereas d is a constant time delay needed for the practical implementation of the communication method. The transceiver circuits were tuned to a regime of robust chaotic behavior. The generated chaotic inter-pulse time intervals $\{T_n\}$ ranged from 10μsec to 25μsec and supported a $\sim$60 kbit/sec bit rate.

The distorted pulses received at the PIN photo detector, placed at the end of the optical propagation path, are applied to the receiver CPPM Rx (see Fig. 1). When the receiver input signal exceeded a chosen threshold level a timer circuit in CPPM Rx was triggered. The receiver acquired two consecutive inter-pulse time intervals T_{n-1} and T_n, which using

$$mS_n = \left[T_n - F(T_{n-1}) - d\right] \tag{2}$$

allows for the decoding of the information signal [11]. Due to the match of the chaotic map $F(\cdot)$ of transmitter and receiver they self-synchronize and the arrival moment of the next pulse can be predicted at the receiver. To improve the system performance by reducing the probability of channel noise falsely triggering the decoder the input of the receiver was blocked until the moment in time when the next pulse was expected.

The turbulent atmospheric channel leads to severe amplitude fluctuations of the received signal, as illustrated by the 200msec timetrace of the received pulse amplitudes shown in Fig. 3a. Despite the significant amplitude fluctuations, the propagation time τ_m, which is the timespan between the leading edge of the TTL pulse applied to the laser and the maximum of the received pulse, only varied within 0.2μsec (see Fig. 3b). Slow and small channel induced pulse propagation time variations are the key to a good performance of the CPPM communication method. However, the detection of the incoming

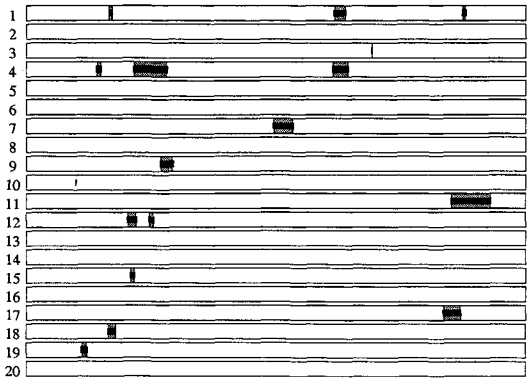

FIGURE 4. Typical structure of errors shown in 20 consecutive measured data streams each of length ~170 msec transmitted at ~2 min intervals. Each strip presents 10000 bits which are transmitted with the CPPM method. White intervals of the strips mark blocks of data received without errors. Narrow black ribbons in the middle of strips mark the blocks of the data received with errors. The gray background shows the blocks of the dropped out data caused by the loss of CPPM pulses due to fading instances.

pulses was implemented using thresholding. The pulse amplitude received by the CPPM Rx circuit had to exceed a certain threshold level (~200mV), which was chosen so as to minimize the probability of CPPM Rx triggering caused by background noise and reflections of optical pulses off nearby surfaces. Consequently, the actual delay time τ_t, measured between the leading edge of the TTL pulses generated by CPPM Tx and the moment of triggering of the CPPM Rx circuit, depends on the amplitude of the received pulses and fluctuates. Due to thresholding τ_t varies (see Fig.3c). The variations however remain smaller than the modulation amplitude $m \approx 1.5\mu$sec and therefore self-synchronization and and communication can be maintained most of the time. Exceptions are the instances of pulse fading (drop-outs), where the received laser beam power falls to the receiver noise level and below the threshold level, respectively. These instances appear as gaps in τ_m and τ_t in Fig. 3.

Voice communication using this free-space communication setup was implemented using delta modulators to digitize an analog microphone signal. Except for the short term (< 50 msec) drop-outs, noticeable as occasional clicks, the voice communication was clear and stable.

Figure 4 shows the structure of lost data in the transmission of binary pseudo-random codes. The total Bit-Error-Rate (BER) measured in the experiment is 1.92×10^{-2}. From Fig. 4 it is apparent that data is lost in blocks and a detailed analysis of the error structure reveals the following main contributions to the BER. First, fading in the channel contributes $\sim 1.78 \times 10^{-2}$ or $\sim 92.7\%$ to the BER. Fading moments, that is instances when pulses do not trigger the CPPM receiver, occur at random times during the communication and are associated with the loss of blocks of data of up to 1000 bits. Second, right before and right after the fading instances the amplitude of the received pulses is still close to the threshold and as consequence even small noise in the channel can result in significant fluctuations of the interpulse intervals (see Fig. 3c). This effect contributes $\sim 1.4 \times 10^{-3}$ to the BER ($\sim 7.3\%$). The rest of the errors, those not related to the complete failure of the communication link due to fading, contribute to the BER only $\sim 5.5 \times 10^{-5}$.

CONCLUSION

We have shown experimentally that the CPPM communication method supports robust data transmission over a turbulent atmospheric channel except for instances when the channel fails due to fading. Due to the self-synchronizing feature of the CPPM method and the fact that the CPPM receiver needs to obtain just two consecutive correct pulses to re-establish the regime of chaos synchronization, the communication after drop-out events is re-established almost immediately.

The authors are grateful to L.S. Tsimring, H.D.I. Abarbanel, L. Larson, and A.R. Volkovskii for helpful discussions. This work was supported in part by U.S. Department of Energy (grant DE-FG03-95ER14516), the U.S. Army Research Office (MURI grant DAAG55-98-1-0269). The authors also thank J. Gowens and J. Carrano for support in the development of the Atmospheric Laser Optics Testbed (A_LOT) at Adelphi, Maryland used in the experiments.

REFERENCES

1. H. Fujisaka and T. Yamada, Prog. Theor. Phys. **69**, 32 (1984); L. M. Pecora and T. L. Carroll, Phys. Rev. Lett. **64**, 821 (1990);
2. D. R. Frey, IEEE Trans. Circuits Syst. **40**, 646 (1993); A. R. Volkovskii and N. F. Rulkov, Tech. Phys. Lett. **19**, 97 (1993); U. Feldman, M. Hasler, and W. Schwarz, Int. J. Ciruit Theory Appl. **24**, 551 (1996); L. Kocarev and U. Parlitz, Phys. Rev. Lett. **74**, 5028 (1995).
3. See, for example, special focus issues: IEEE Trans. Circuits Syst. **48** No. 12 (2001); Chaos **6** No. 3 (1996); Chaos **7** No. 4 (1997); Int. J. Bif. Chaos **10**, No. 11&12 (1993); Int. J. Circuit Theory Appl. **27** (1999);.
4. G. Kolumban, M. P. Kennedy and L. O. Chua, IEEE Trans. Circuits Syst. **45**, 1129 (1998); C. Williams, IEEE Trans. Circuits Syst. **48**, 1394 (2001).
5. T. L. Carroll, Phys. Rev. E **53** 3117 (1996); T. L. Carroll and G. A. Johnson, Phys. Rev. E **57** 1555 (1998); E. Rosa, S. Hayes, and C. Grebogi, Phys. Rev. Lett. **78** 1247 (1997); H. Torikai, T. Saito, and W. Schwartz, IEEE Trans. Circuits Syst. **46**, 1072 (1999).
6. T. L. Carroll, IEEE Trans. Circuits Syst. **42**, 105 (1995); IEEE Trans. Circuits Syst. **48**, 1519 (2001); N. F. Rulkov and L. Tsimring, Int. J. Circuit Theory Appl. **27**, 555 (1999);
7. Backscatter enhancement effects result from correlations in the wavefront phase aberrations between the outgoing and the returned waves which propagate through the same refractive index inhomogeneities [8]. The variance characterizing the received wave phase and intensity fluctuations can exceed the corresponding value for a unidirectional wave that propagates a distance $z = 2L$ by more than a factor of two under strong scintillation conditions [8, 9].
8. L. C. Andrews, R.L. Phillips, and C.Y. Hopen,*Laser Beam Scintillation with Applications*, (SPIE Press, Bellingham, 2001).
9. Yu. A. Kravtsov and A.I. Saichev,*Sov. Phys. Usp.*, **25**, 494 (1982).
10. M. M. Sushchik, *et al. IEEE Communication Letters*, **4**, 128 (2000); N. F. Rulkov, *et al. IEEE Trans. Circ. Syst.* **48**, 1436 (2001).
11. In the CPPM Tx and CPPM Rx devices the consecutive values of T_n and T_{n-1} are generated and stored in the form of voltage signals. Eqs. (1) and (2) are implemented using an analog electrical circuit of the nonlinear function $F(.)$ and a subtracting circuit, see Ref. [10] for details.